Aberrant theta-gamma frequency coupling in patients with first episode psychosis

초발 정신증 환자에서 세타-감마 주파수 연결성 이상에 관한 연구

August 2019

**Graduate School of Seoul National University
Department of Brain and Cognitive Sciences**

Tak Hyung Lee

Aberrant theta-gamma frequency coupling in patients with first episode psychosis

Advisor: Jun Soo Kwon

Submitting a Ph.D. Dissertation of Public Administration

August 2019

Graduate School of Seoul National University
Department of Brain and Cognitive Sciences

Tak Hyung Lee

Confirming the Ph.D. Dissertation written by
Tak Hyung Lee
August 2019

Chair	_____	(Seal)
Vice Chair	_____	(Seal)
Examiner	_____	(Seal)
Examiner	_____	(Seal)
Examiner	_____	(Seal)

Abstract

Background: Although cognitive dysfunction has been suggested as one of the core pathologies of schizophrenia and affects patients' daily functioning and quality of life, little is known about its neurobiological underpinnings, which would lead to and instigate the development of effective treatment methods. Since the resting-state activity is crucial for cognitive functioning and electroencephalography (EEG) can reflect moment-by-moment changes of neural activity with high temporal resolution, I aimed to investigate theta phase-gamma amplitude coupling (TGC) of resting-state EEG and its relationship with cognitive functioning in patients with first episode psychosis (FEP).

Methods: A total of 59 FEP patients and 50 healthy controls (HCs) participated in the resting-state EEG recording in eyes-closed state. In addition, the Trail Making Test Part A (TMT-A) and Part B (TMT-B), and the California Verbal Learning Test (CVLT) were used to measure cognitive functioning. The TGC from standardized low-resolution brain electromagnetic tomography (sLORETA) source signal of resting-state EEG was calculated in the default mode network (DMN)-related brain regions and was compared between the FEP and HC groups. Correlation analyses to reveal the relationship between TGC in FEP patients and the performance of neurocognitive function tests (NCFTs) were conducted.

Results: Mean resting-state TGC was larger for the FEP group than for HCs. Patients with FEP showed greater TGC in the left posterior cingulate cortex (PCC), which was correlated with better performances in TMT-A and TMT-B, and with the immediate and delayed recall of the CVLT.

Conclusion: Larger TGC in the brain regions comprising DMN in the FEP group

compared to HCs indicates that patients with FEP may show compensatory hyperactivation of DMN-related brain regions during the resting-state, which may be related with reallocation of cognitive resources for preparing cognitive execution. This study not only highlights the moment-by-moment neural underpinnings of cognitive dysfunction in FEP patients but also provides useful background and insight in developing treatment methods for cognitive dysfunction of schizophrenia.

Keyword : cross frequency coupling, default mode network, electroencephalography, theta phase-gamma amplitude coupling, resting-state

Student Number : 2015-30988

Table of Contents

Chapter 1. Introduction

Schizophrenia and cognitive dysfunction

Patients with schizophrenia suffer from positive and negative symptoms such as delusion, hallucination, anhedonia, and social withdrawal. In addition to psychotic symptoms, significant cognitive dysfunction affects patients' daily functioning and quality of life from the early to chronic stage of the disorder (Alptekin et al., 2005; Kahn and Keefe, 2013; Sheffield and Barch, 2016; Ueoka et al., 2011). Schizophrenia patients show impairments in various domains of cognitive functioning including episodic memory, working memory, executive function, learning, and processing speed (Meier et al., 2014; Mesholam-Gately et al., 2009). Those are also closely related to psychotic symptoms, because negative symptoms are associated with dysfunctions in verbal fluency, memory, and learning, and disorganization symptoms are related to low intelligent quotient (IQ; O'Leary et al., 2000).

However, it has been reported that cognitive dysfunction persisted after successful treatment which led to the improvement of psychotic symptoms, and those persistent cognitive dysfunctions had a significant negative effect on the quality of life and prognosis for patients with schizophrenia (Alptekin et al., 2005; Ueoka et al., 2011). Despite the significance of cognitive functioning in the psychotic symptoms, daily life, and prognosis of schizophrenia, current treatments including antipsychotic medication, neuromodulation, and cognitive-behavioral therapy have not been successful enough (Goff et al., 2011; Palm et al., 2016; Tripathi et al., 2018). That may be, at least partially, due to the insufficient understanding of treatment

targets (i.e. neural mechanism underlying cognitive dysfunctions). Therefore, neural correlates of cognitive dysfunctions in patients with schizophrenia are required to be further investigated in order to inform the development of effective treatments for the improvement of cognitive functioning.

Resting-state and cognitive function in schizophrenia

Brain activity in the resting-state plays an important role in cognitive functioning. Previous studies on human brain and cognition have primarily focused on the brain areas in which the signal change was manifested during the performance of a particular cognitive task (Buckner et al., 2008; Li et al., 2015; Vlahou et al., 2014). In contrast to common beliefs that the task-performing brain requires more energy, the human brain consumes up to 80% of the energy at the resting-state, while only 5 to 10% of the energy is required for task performance (Raichle and Mintun, 2006). Therefore, we can assume that many neural activities occur during the resting-state.

Studies using functional magnetic resonance imaging (fMRI) found that blood-oxygen-level-dependent (BOLD) signal of various brain regions changed with mutual relationship in the resting-state (Raichle et al., 2001), known as resting-state network. The most consistently reported resting-state network is the default mode network (DMN) which has a significant impact on cognitive functioning (Van Den Heuvel and Pol, 2011). The brain areas comprising the DMN include the medial prefrontal cortex (mPFC), posterior cingulate/retrosplenial cortex (PCC/Rsp), inferior parietal lobule (IPL), and medial temporal cortex (Smith et al., 2018). DMN is related to various cognitive functions including integration of cognitive and emotional processing (Greicius et al., 2003), monitoring the world around us

(Gusnard and Raichle, 2001), stimulus independent thoughts (Mason et al., 2007), and integration of internal and external information (Smith et al., 2018). DMN showed relatively reduced activity during task execution, suggesting that DMN plays an important role in the preparation of task performance and in the modulation of switching from the resting-state to the task performance state (Buckner et al., 2008; Smith et al., 2018).

The "dysconnection hypothesis" explains abnormal functional integration between brain regions, manifested at the level of modulation of associate changes in synaptic efficacy, as a main pathophysiological mechanism of psychotic symptoms and cognitive dysfunctions found in patients with schizophrenia (Friston, 1998; Friston et al., 2016; Pettersson-Yeo et al., 2011). Because resting-state neural activity is important not only for psychotic symptoms but also for cognition, many studies have investigated resting-state connectivity in schizophrenia patients to reveal neural correlates of cognitive dysfunction (Anticevic et al., 2012; Hunt et al., 2017; Karbasforoushan and Woodward, 2012). The hyperactivation or hyperconnectivity of the brain regions comprising the DMN has been reported in patients with schizophrenia (Hunt et al., 2017), while other studies have shown hypoactivation or hypoconnectivity of DMN related brain regions (Bluhm et al., 2007; Pankow et al., 2015). This altered functional connectivity (FC) showed significant relationship with various cognitive functioning in patients with schizophrenia (Bassett et al., 2012; Cole et al., 2011; Unschuld et al., 2014; Wang et al., 2014). For example, Cole et al. found that larger resting-state FC of the PFC to other brain regions was associated with poorer performance in working memory task (Cole et al., 2011; Unschuld et al., 2014). Similarly, Wang et al. reported a positive correlation between the resting-state long range FC of the precuneus and the processing speed (Wang et al., 2014). In

addition, it was shown that smaller network organization during resting-state was associated with poorer attention and memory in patients with schizophrenia (Bassett et al., 2012).

Although many fMRI studies reported FC of DMN-related brain regions as a neural correlate of cognitive dysfunction in patients with schizophrenia, its low temporal resolution cannot explain the moment-by-moment changes of neural activity during the resting-state. Electroencephalography (EEG) is a superior approach to cognitive processing during the resting-state because EEG has very high temporal resolution at the millisecond level (Bell et al., 1992). For example, Khanna et al. suggested microstate analysis of resting-state EEG to investigate changes in neural activity in every moment, which was called "the atoms of thoughts" (Khanna et al., 2015). Therefore, EEG which shows very high temporal resolution is optimally suitable to investigate neural correlates of cognitive dysfunction in schizophrenia patients during the resting-state.

However, such studies using EEG showed low spatial resolution, therefore EEG could not be used for the investigation of localization-based brain networks (He et al., 2011). Since the EEG signal is measured from the outer surface of the head, it is difficult to know the exact location in the brain where neural activity occurs, but EEG can be complemented with source analysis with structural information acquired with MRI (Mantini et al., 2007; Yuan et al., 2016). In a simultaneous EEG and fMRI study, EEG-derived resting-state networks was significantly correlated with resting-state networks constructed from fMRI data (Yuan et al., 2016). However, the EEG band power spectrum patterns of each resting-state fMRI network was found to be different from each other (Mantini et al., 2007). Therefore, investigation of a spatiotemporal psychopathology using the source analysis of resting-state EEG data

4

was proposed to estimate both temporal and spatial features of the neural substrate of pathophysiology of schizophrenia (Cabral et al., 2014; Northoff and Duncan, 2016).

Neural oscillation and theta phase-gamma amplitude coupling (TGC)

Neural oscillations occur at different frequencies depending on layers and conditions in most cortical regions (Wang, 2010). Several types of neural oscillations occur with specific coupling between different frequencies (Jensen and Colgin, 2007). Each oscillation has three features; frequency, amplitude, and phase. In theory, two different features can be combined, thus four combinations of cross-frequency coupling (CFC) functions are possible; phase-frequency coupling, phase-phase coupling, phase-amplitude coupling, and amplitude-amplitude coupling (Hyafil et al., 2015; Jensen and Colgin, 2007). The CFC functions are related with information processing such as multi-item/sequence representation, long-distance communication, sensory parsing, and de-multiplexing (Uhlhaas et al., 2008). CFC processes information by modulating the amplitude of the fast oscillating activity on the basis of phase of the slow oscillating activity, and among CFCs, theta phase-gamma amplitude coupling (TGC) has been the most widely studied (Lisman and Jensen, 2013).

TGC provides a mechanism for information processing and communication coordination between brain regions (Canolty and Knight, 2010; Lisman and Jensen, 2013). The most widely known role of TGC is the phase precession that occurs when spatial information is processed in the hippocampus (Lisman and Jensen, 2013). Animal studies have shown that gamma activity occurred in a certain phase of theta when rats were in a specific position while moving, and that the phase of theta

coupled with gamma activity was related to the presentation of spatial information (Battaglia, 2004; Wilson et al., 2002). In addition, increased accuracy during spatial information learning was accompanied by increased TGC, suggesting that TGC was also related to the recall of spatial memory and learning process (Tort et al., 2009). In humans, intracranial EEG recording during working memory task performance showed that TGC increased in accordance with increasing cognitive load (Axmacher et al., 2010). In addition, theta coherence between brain regions increased at a certain point during a task performance (Benchenane et al., 2010; Kim et al., 2011), therefore, it was suggested that gamma oscillation changes related to the timing of theta oscillation (i.e. TGC) may be related to information transfer in the brain (Lisman and Jensen, 2013).

In patients with schizophrenia, whose cognitive dysfunctions have been known to be one of the core symptoms, abnormal TGCs have been consistently reported (Barr et al., 2017; Popov et al., 2015). Especially, hypofunctioning N-methyl-D-aspartate (NMDA) receptor and decreased gamma amino butyric acid (GABA) mediated signaling have been suggested as the molecular mechanisms of cognitive dysfunction in schizophrenia in relationship with TGC abnormality (Kahn and Sommer, 2015). Because the abnormal NMDA-GABAergic system causes disturbance of neural oscillations, especially in the gamma and theta frequencies (Uhlhaas and Singer, 2015), TGC has been suggested as a new approach to reveal the neural correlate of cognitive dysfunction in schizophrenia (Lisman and Buzsáki, 2008). Most previous studies using TGC in patients with schizophrenia measured TGC during a specific task performance (Barr et al., 2017; Lynn and Sponheim, 2016; Popov et al., 2015). During a working memory task performance, healthy volunteers showed increased TGC according to the increasing cognitive load; however,

schizophrenia patients did not show those changes, suggesting that schizophrenia patients had impairments in modulating the function of TGC in response to different cognitive loads (Barr et al., 2017). In addition, schizophrenia patients showed reduced TGC during the Stroop task performance, indicating dysfunctions in interference control or set shifting (Popov et al., 2015). However, despite the importance of resting-state neural activity in overall cognitive functioning, the number of studies investigating TGC during resting-state in patients with schizophrenia is limited. Recent research by Won et al. showed that resting-state TGC was larger in schizophrenia patients compared to healthy controls (HCs) and distinguished patient and HC groups more accurately than power spectrum results (Won et al., 2018).

Aims and hypothesis

Unraveling the moment-by-moment neural correlates of cognitive dysfunction in patients with schizophrenia would not only provide deeper understanding of schizophrenia pathophysiology but also promote the development of effective treatments for cognitive dysfunction. To investigate the spatiotemporal neural correlates of cognitive dysfunction in schizophrenia, I performed source analysis of resting-state TGC in the brain areas comprising DMN and compared TGCs between patients with first episode psychosis (FEP) and HCs. Investigating FEP patients is advantageous because it minimizes the effect of age, illness duration, medication exposure, disease chronicity, which significantly confound EEG results in chronic patients. The correlation between TGC and performances during neurocognitive function tests (NCFT) in each group of participants was also estimated. I hypothesized that FEP patients would show increased TGC in brain

regions comprising DMN and altered TGC would show a significant relationship with behavioral performance of NCFT.
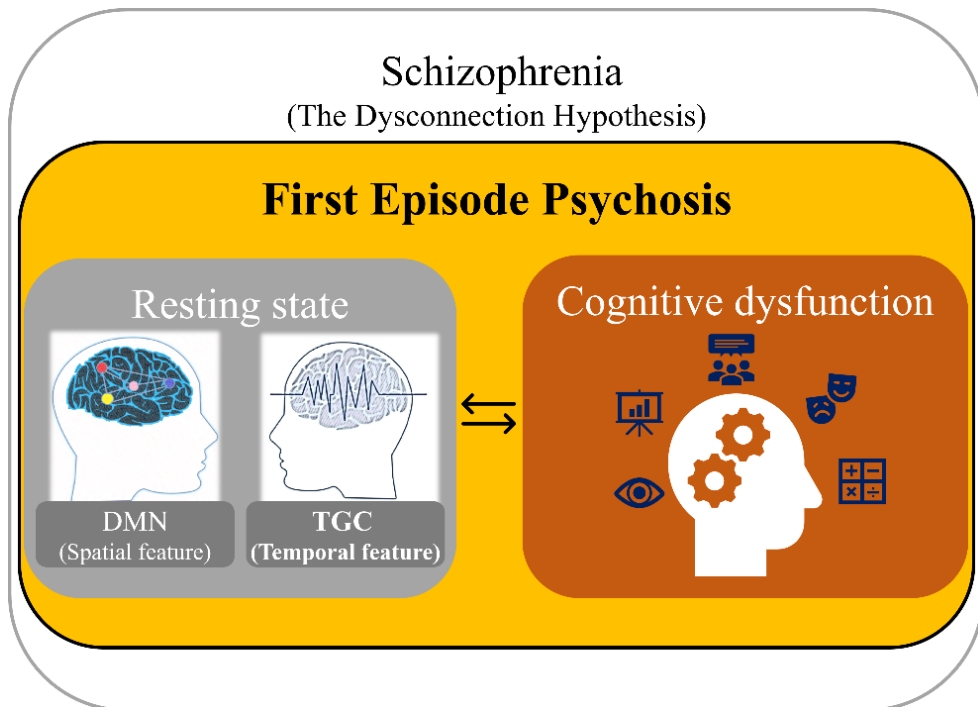

Figure 1. Summary of the introduction. DMN, default mode network; TGC, theta phase-gamma amplitude coupling.

Chapter 2. Methods

Participants

Fifty-nine patients with FEP and 50 HCs participated in this study. Inpatient and outpatient FEP patients were recruited from the Seoul National University Hospital (SNUH) and the Seoul Youth Clinic, a center for the prospective, longitudinal investigation of people in the early phase of psychotic disorder (Kwon et al., 2012). FEP patients were defined as patients diagnosed with schizophrenia, schizoaffective disorder, or schizophreniform disorder within the past two years using the Structured Interview for the Diagnostic and Statistical Manual of Mental Disorders, Fourth Edition Axis I Disorders (SCID-I). The severity of clinical symptoms and general functional status were assessed using the Positive and Negative Syndrome Scale (PANSS) and the Global Assessment of Functioning (GAF) scale, respectively, by experienced psychiatrists. Recruitment of HCs was conducted via internet advertisement. HCs were excluded in case of current diagnosis or history of DSM-IV Axis I psychiatric disorders, or if there was a patient with psychotic disorder within third-degree relatives in the family. Common exclusion criteria for both FEP and HC groups included history of substance abuse or dependency (except for nicotine), severe head trauma or neurological disease, severe medical illness, sensory impairments such as auditory or visual impairments, or intellectual disability (IQ < 70).

This study was conducted in accordance with the Declaration of Helsinki and the study protocol was approved by the Institutional Review Board of SNUH. All study participants fully understood the study procedures and provided written informed consent. For minors, additional written informed consent was obtained

from their parents.

Neurocognitive function tests

Patients with FEP and HCs participated in the set of NCFT. Trail Making Test, Part A (TMT-A) and Part B (TMT-B) were used to measure attention and working memory, respectively. Verbal memory was assessed using the Korean version of California verbal learning test (CVLT) in which immediate recall of 16 words from 4 semantic categories and delayed recall after 20 minutes were also evaluated.

EEG acquisition and pre-processing

Continuous resting-state EEG data were recorded using the SynAmps2 with 128 channel Quik-Cap based on the modified international 10-20 system (Figure 2). Vertical and horizontal electro-oculogram electrodes were placed below and on the outer canthus of the left eye to measure eye movement artifacts. The ground electrode was placed on AFz and a linked mastoid electrode served as a reference electrode. The bandwidth of the hardware filter was set to 100 Hz from direct current (DC), and the sampling rate was 1000 Hz. The impedance of all electrodes was maintained under 5 kOhm. EEG data were recorded for 2 or 5 minutes in an eye-closed resting-state in a dim lit, quiet, and electrically shielded room.
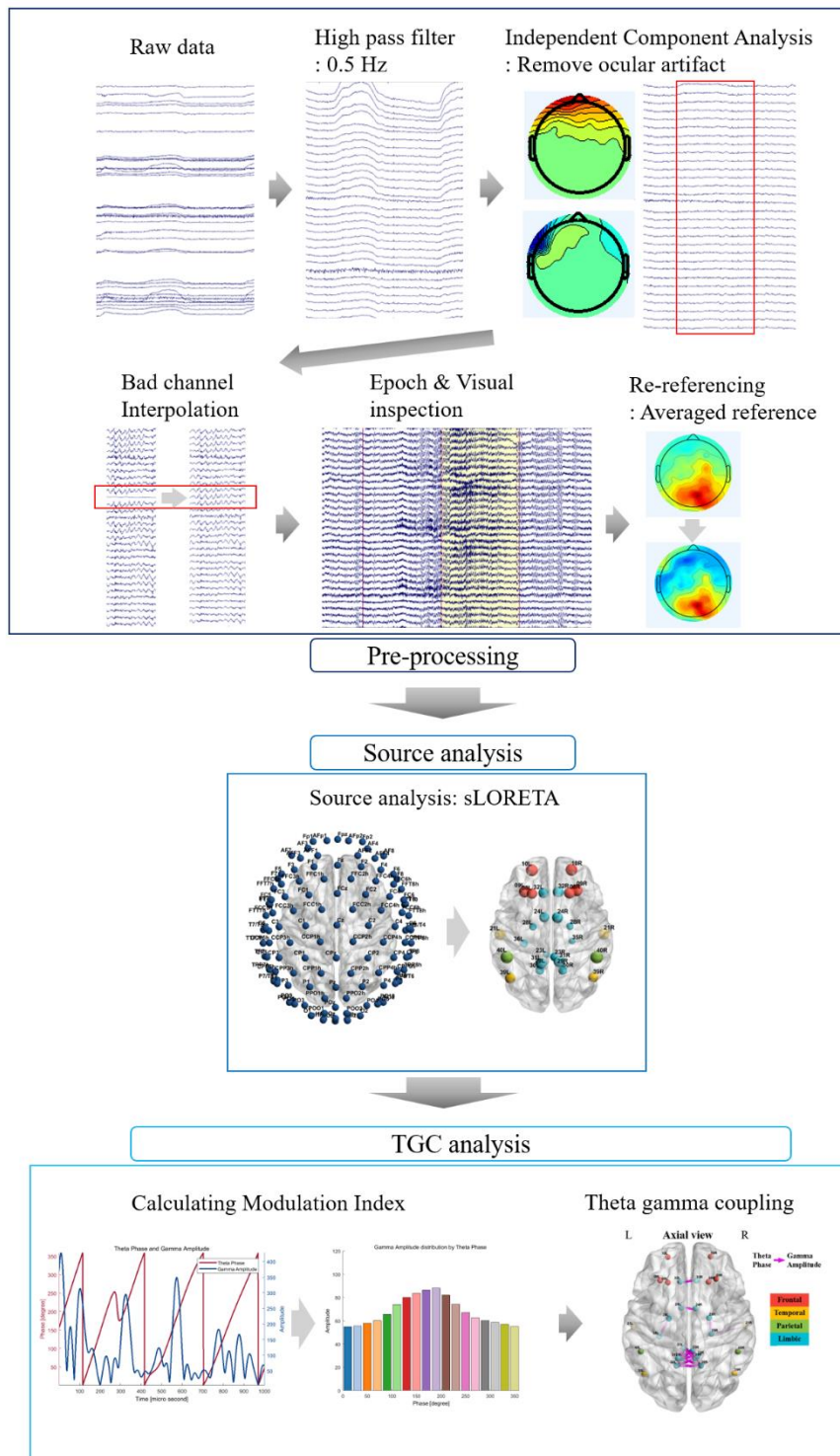
Figure 2. The electroencephalography electrodes montage mapped onto the standardized Montreal Neurological Institute (MNI) space.

Pre-processing of data was performed using MATLAB R2017a (Mathworks, USA) and the EEGLAB toolbox (Delorme and Makeig, 2004). The pipeline of the pre-processing procedure is shown in Figure 3. Continuous EEG data were filtered using a 0.5-Hz high-pass filter, and then independent component analysis (ICA) using the second order blind identification (SOBI) algorithm embedded in EEGLAB was performed to eliminate artifacts (Belouchrani and Cichocki, 2000; Urigüen and Garcia-Zapirain, 2015). The ocular artifact and electrocardiographic components were selected using the SASICA toolbox (Chaumon et al., 2015) and visual inspection. Bad channel electrodes were interpolated, and the maximum number was less than 7 in each subject. After re-referencing using an average reference, continuous EEG data was divided into 4-second epochs. Finally, additional visual inspection was performed to remove residual artifacts.

Figure 3. The pipeline of data processing.

Source analysis

EEG source analysis was performed using the standardized low resolution electromagnetic tomography (sLORETA) method with the LORETA-KEY alpha-software program (Pascual-Marqui, 2002). Pre-processed data were aligned with the electrode template embedded in the LORETA-KEY alpha-software, and the source signal for the entire data was analyzed. In order to extract the source area corresponding to the DMN, we selected 28 regions of interest (ROIs) based on the Brodmann area (BA) information included in the DMN (Buckner et al., 2008; Thatcher et al., 2014). Source signals were extracted from the centroid voxel of each BA. The 28 BA ROIs comprising the DMN and the Montreal Neurological Institute (MNI) coordinates of centroid voxel of each ROI are shown in Table 1 and Figure 4.
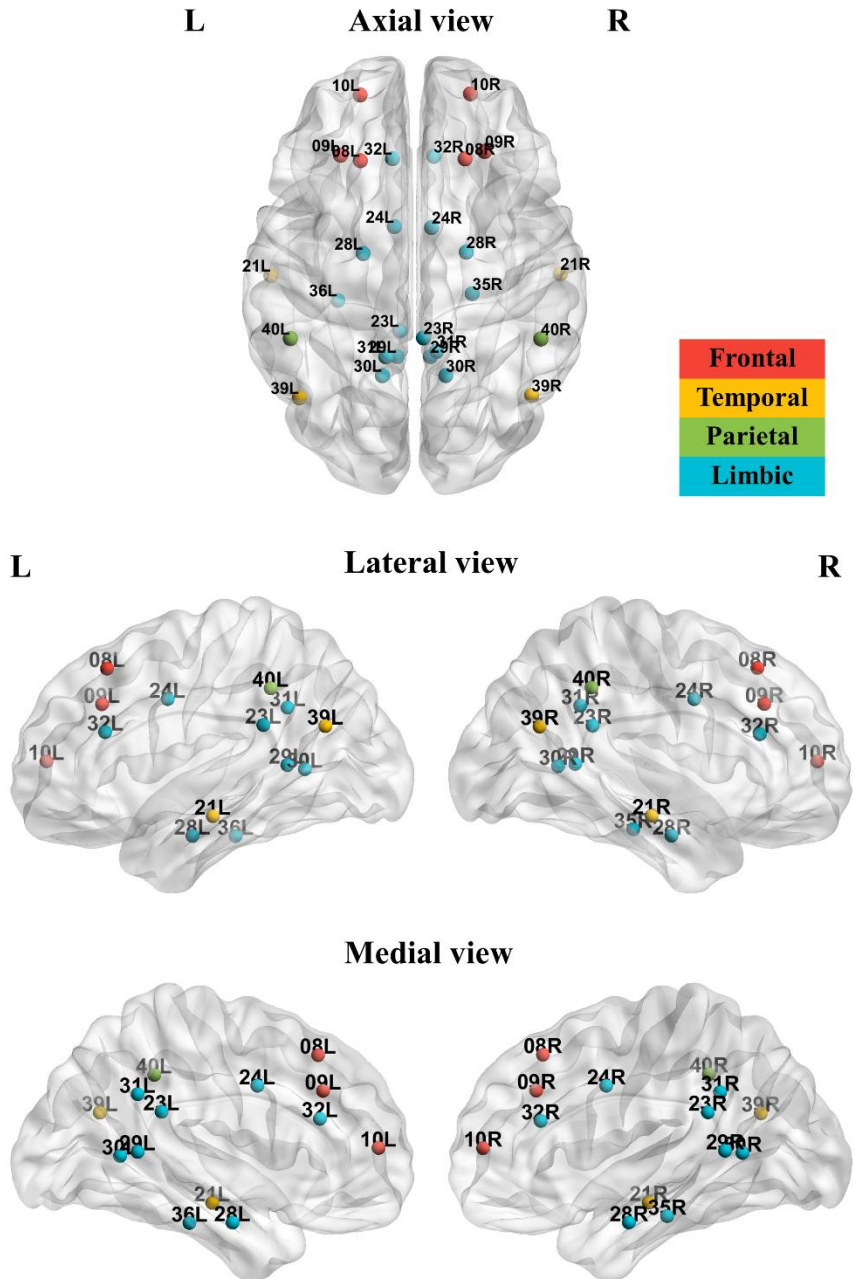
Figure 4. Regions of interest comprising the default mode network. L, Left; R, Right.

Table 1. Montreal Neurological Institute (MNI) coordinates of centroid voxel in each Brodmann area (BA) comprising the default mode network (Buckner et al., 2008).

Brodmann area	MNI coordinate			ROI
	X	Y	Z	
Brodmann area 8	-20	30	50	BA08L
Brodmann area 9	-30	30	35	BA09L
Brodmann area 10	-25	55	5	BA10L
Brodmann area 21	-60	-20	-15	BA21L
Brodmann area 28	-20	-10	-25	BA28L
Brodmann area 36	-30	-30	-25	BA36L
Brodmann area 23	-5	-40	25	BA23L
Brodmann area 24	-5	0	35	BA24L
Brodmann area 32	-5	30	20	BA32L
Brodmann area 29	-5	-50	5	BA29L
Brodmann area 30	-15	-60	5	BA30L
Brodmann area 31	-10	-50	30	BA31L
Brodmann area 39	-45	-65	25	BA39L
Brodmann area 40	-50	-40	40	BA40L
Brodmann area 8	20	25	50	BA08R
Brodmann area 9	30	30	35	BA09R
Brodmann area 10	25	55	5	BA10R
Brodmann area 21	60	-15	-15	BA21R
Brodmann area 28	20	-10	-25	BA28R
Brodmann area 35	30	-25	-25	BA35R
Brodmann area 23	5	-45	25	BA23R
Brodmann area 24	5	0	35	BA24R
Brodmann area 32	5	30	20	BA32R
Brodmann area 29	5	-50	5	BA29R
Brodmann area 30	10	-60	5	BA30R
Brodmann area 31	10	-50	35	BA31R
Brodmann area 39	45	-65	25	BA39R
Brodmann area 40	50	-45	45	BA40R

Abbreviation: L, left; R, right; ROI, region of interest.

Theta phase-gamma amplitude coupling

TGC was analyzed using the MATLAB and EEGLAB functions as a modulation index (MI) (Tort et al., 2010). In order to obtain MI, source data were converted into several frequency bands including theta (4~7 Hz) and gamma (30~50 Hz) range using the basic finite impulse response filter implemented in EEGLAB. The analytic signal amplitude of the gamma band and the phase of theta band were obtained by Hilbert transform. The phase of theta band was divided into 18 bins with a range of 20 degrees, and the average of the gamma band amplitudes corresponding to each bin was calculated (a representative example is shown in Figure 5). When gamma amplitude is the same in all phase bins, MI becomes 0. When gamma amplitude is larger in the narrow range of phase bins, MI becomes closer to 1. When the data length is short, MI is more influenced by the input data length, thus 100 seconds data were used for the analysis to obtain a fair MI value. MI and ROI locations were visualized with the BrainNet viewer (Xia et al., 2013).
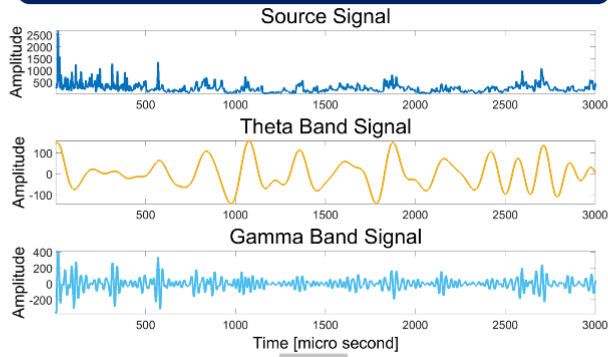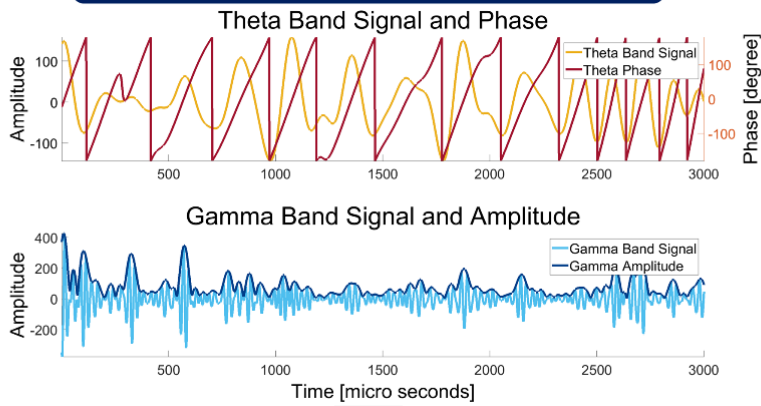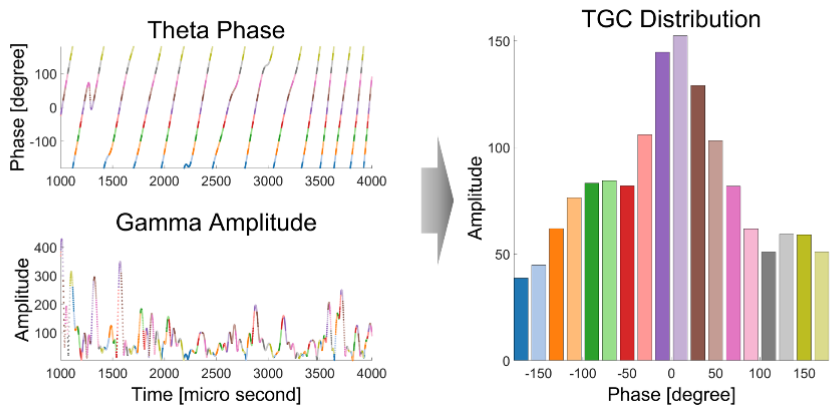
Figure 5. The calculation process of theta phase-gamma amplitude coupling. In this example, 3 seconds data were used for visualization.

Statistical analysis

Statistical analysis was performed using R and MATLAB. Independent samples t-test was used to reveal group difference of age, IQ, education years, and the results of neurocognitive function tests. For the comparison of categorical data such as sex and handedness, a chi-square test was conducted. Permutation tests were performed on the EEG data of each individual to verify that TGC was actually present in each intra- or inter-ROI. For the permutation test, each theta phase and gamma amplitude data of 4 seconds obtained from 25 epochs in each individual ROI was randomly matched on 1000 iterations and MI distribution was calculated. Using this distribution, the MI of actual data was evaluated for significant differences. TGC comparisons between groups were performed using the significant ROI combinations found in all individuals through the permutation test. General linear model with age and sex as covariates was conducted to show group differences between TGC values. For multiple comparison correction, false discovery rate (FDR) was used. Partial correlation analysis with age and sex as covariates was performed to reveal the relationship between TGC of ROI combinations, which showed significant group differences, and clinical measures such as symptomatic severity or neurocognitive functioning. p-values below 0.05 were considered significant for all statistical analyses

Chapter 3. Results

Characteristics of the participants

Demographic and clinical characteristics as well as the results of NCFT of patients with FEP and HCs are summarized in Table 2. There was no significant difference between groups in age, handedness, and education years. However, there were more females ($\chi2 = 9.026$, P = 0.003) in the FEP group, and patients with FEP had lower IQ (t = −5.766, P<0.001) compared to HCs. Patients with FEP performed more poorly in all NCFTs than HCs; TMT-A (t = −2.613, P = 0.012), TMT-B (t = 3.564, P = 0.001), CVLT-immediate recall (t = −4.295, P<0.001), CVLT-delayed recall (t = −4.942, P<0.001).

Table 2. Demographic and clinical characteristics and neurocognitive function tests.

	FEP n=59	HC n=50	T or χ^2	P
Demographic characteristics				
Age	23.2 (4.9)	22.7 (4.4)	0.522	0.606
Sex (Male/Female)	22/37	34/16	9.026	0.003*
Handedness (Right/Left)	54/5	47/3	0.016	0.900
Education year	13.8 (2.2)	14.2 (1.7)	-0.840	0.403
IQ	100.7 (13.5)	115.5 (13.3)	-5.766	< 0.001**
Clinical characteristics				
PANSS Total[a]	62.3 (16.7)			
PANSS Positive[a]	15.1 (5.4)			
PANSS Negative[a]	15.8 (5.7)			
PANSS General[a]	31.4 (8.9)			
GAF[b]	50.4 (14.3)			
Neurocognitive function test				
TMT-A[c]	28.1 (13.4)	22.0 (6.8)	2.613	0.012*
TMT-B[c]	72.6 (31.4)	53.0 (16.0)	3.564	0.001*
CVLT, immediate recall[d]	9.8 (3.7)	12.9 (2.9)	-4.295	<0.001**
CVLT, delayed recall[d]	10.1 (3.6)	13.4 (2.5)	-4.942	<0.001**

Abbreviations: FEP, first episode psychosis; HC, healthy control; IQ, intelligent quotient; TMT – A, trail marking test, part A; TMT – B, trail marking test, part B; CVLT, California verbal learning test.
[a] The number of missing data was 3 in patients with FEP.
[b] The number of missing data was 1 in patients with FEP.
[c] The number of missing data was 20 in patients with FEP.
[d] The number of missing data was 19 in patients with FEP.
* P <0.05, ** P <0.001.

Theta-gamma coupling results

Permutation test revealed that local TGCs of 28 ROIs were significant in all individuals and thus confirmed as TGCs that were actually present (Figure 6). TGC combinations between ROIs were excluded from further analysis because they were likely to appear due to volume conduction as they were in close proximity to each other. Mean values of TGCs from 28 ROIs showed that MI of patients with FEP was higher (t = 2.63, P = 0.010) than that of HCs (Figure 7).
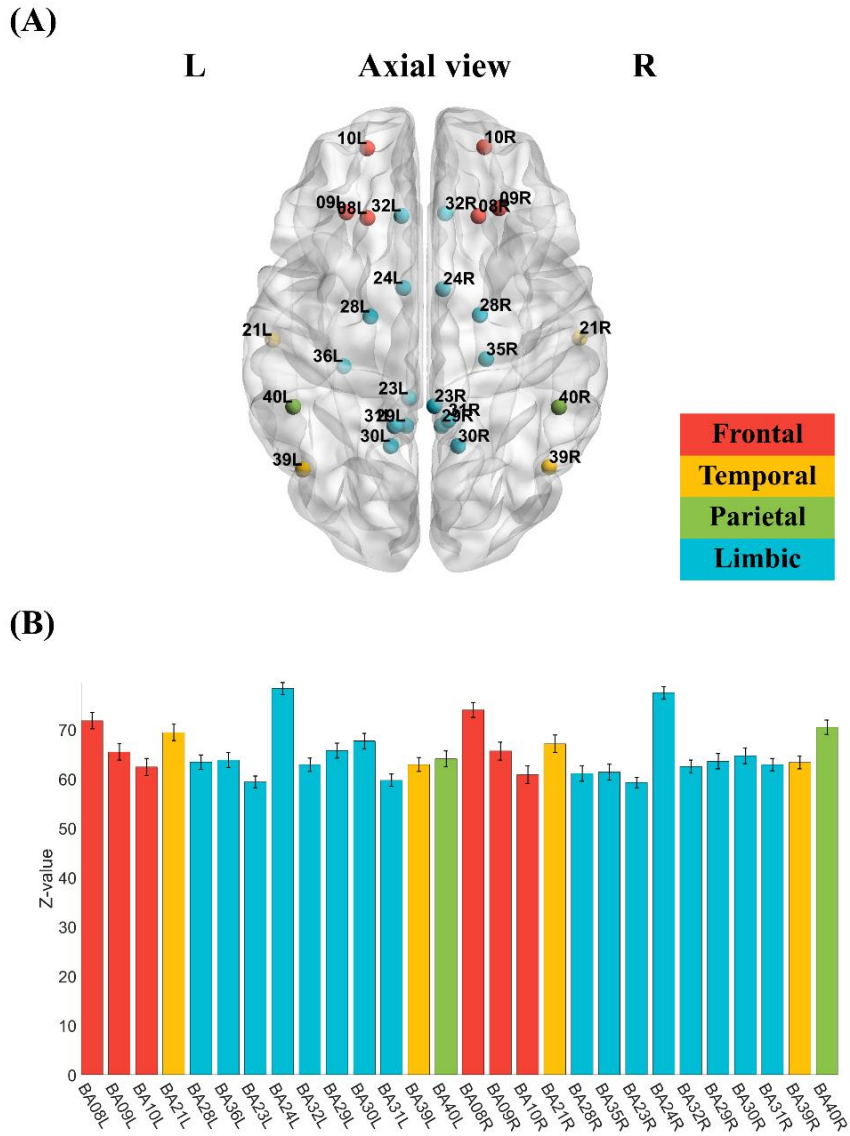
(A)

(B)

Figure 6. Summary of the permutation test results. The color of each region of interest (ROI) indicates structural location. (A) ROIs of significant theta-gamma coupling found in all individuals. (B) Mean Z-value based on the permutation test results. Error bar indicates standard error. Abbreviation: BA, Brodmann area; L, Left; R, Right.
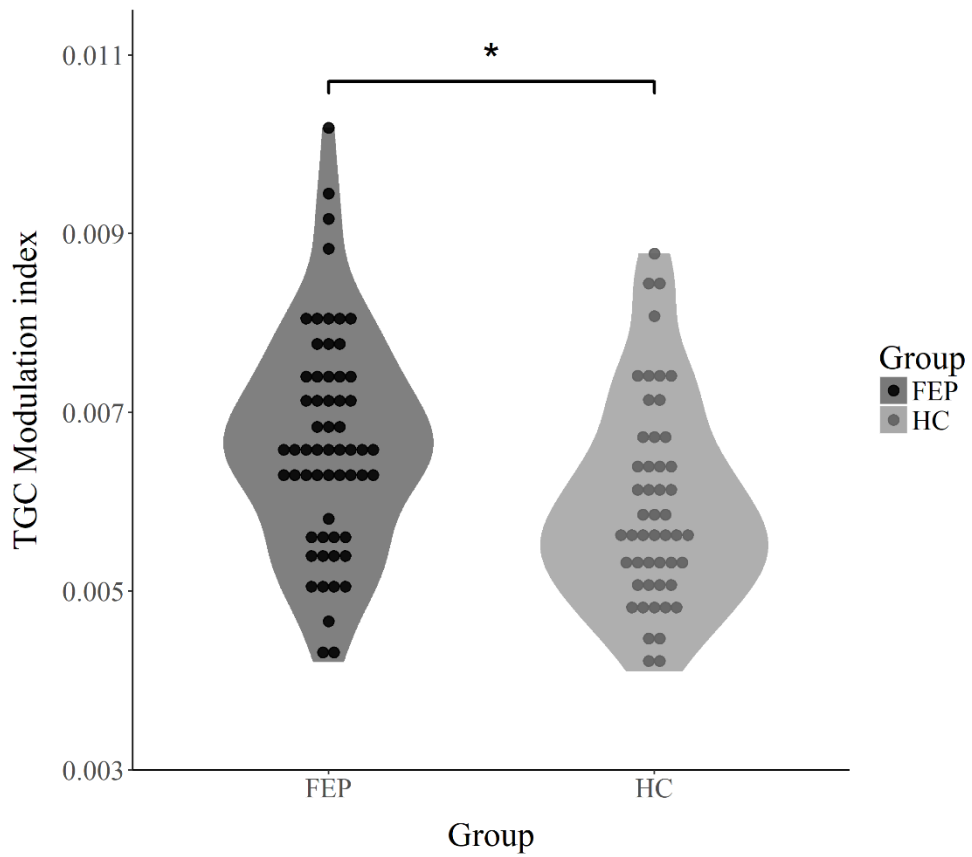
Figure 7. Group comparison of theta-gamma coupling (TGC) between patients with first episode psychosis (FEP) and healthy control (HC) individuals. Error bars represent standard errors of the means. *: P < 0.05.

In order to reveal specific ROIs with higher TGC in FEP patients, we compared TGC for each ROI combination and performed FDR correction for controlling for multiple comparisons. After FDR correction, two TGCs were significantly different between FEP and HC groups. Local TGC differences were found in the BA29L (t=3.303, P_{FDR}=0.018) and the BA30L (t=4.120, P_{FDR}=0.002), which comprise the left posterior cingulate cortex (PCC). Results are summarized and shown in Figure 8, Figure 9, and Table 3.
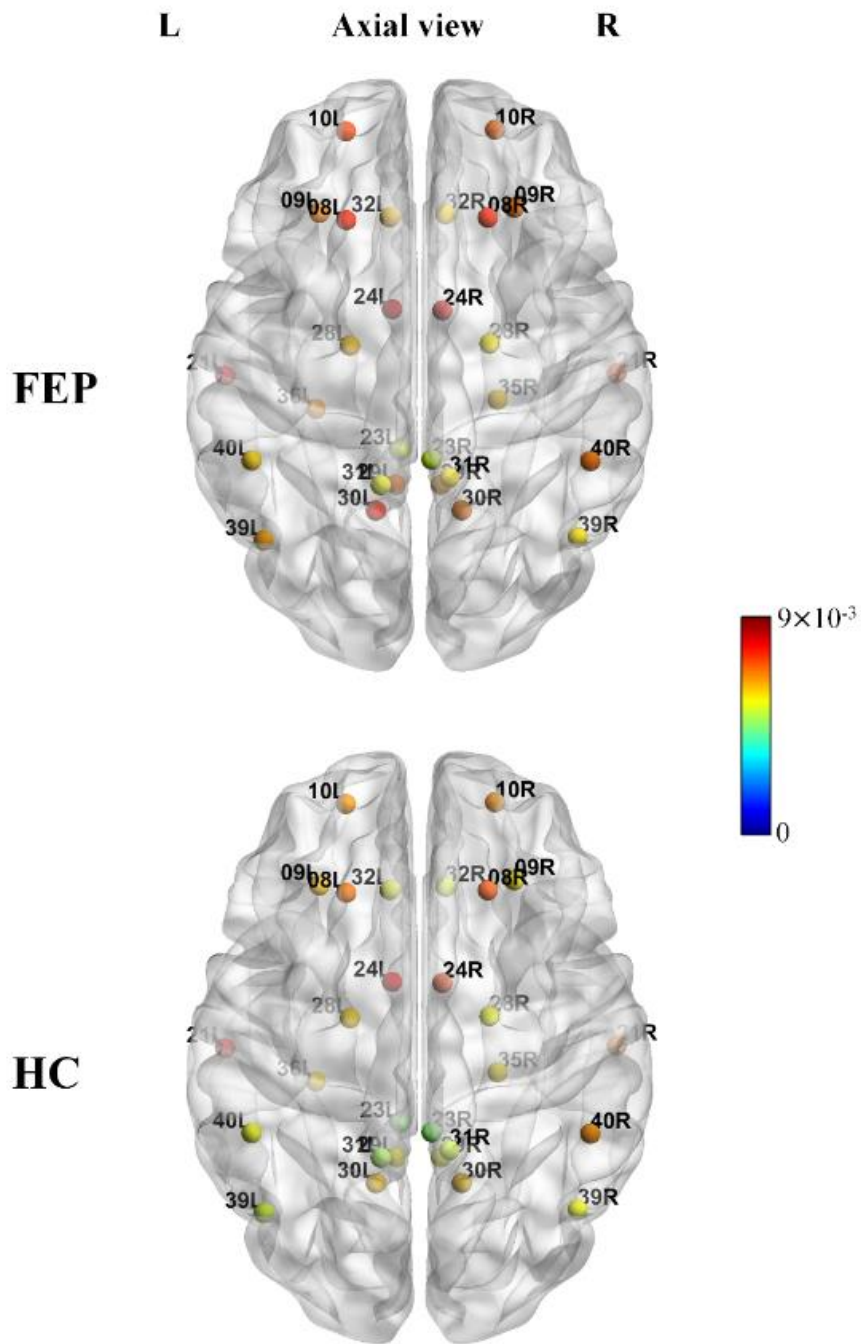
Figure 8. The group average theta phase -gamma amplitude couplings (TGC) of each ROI. The color of ROI indicates the TGC average value. L, Left; R, Right.
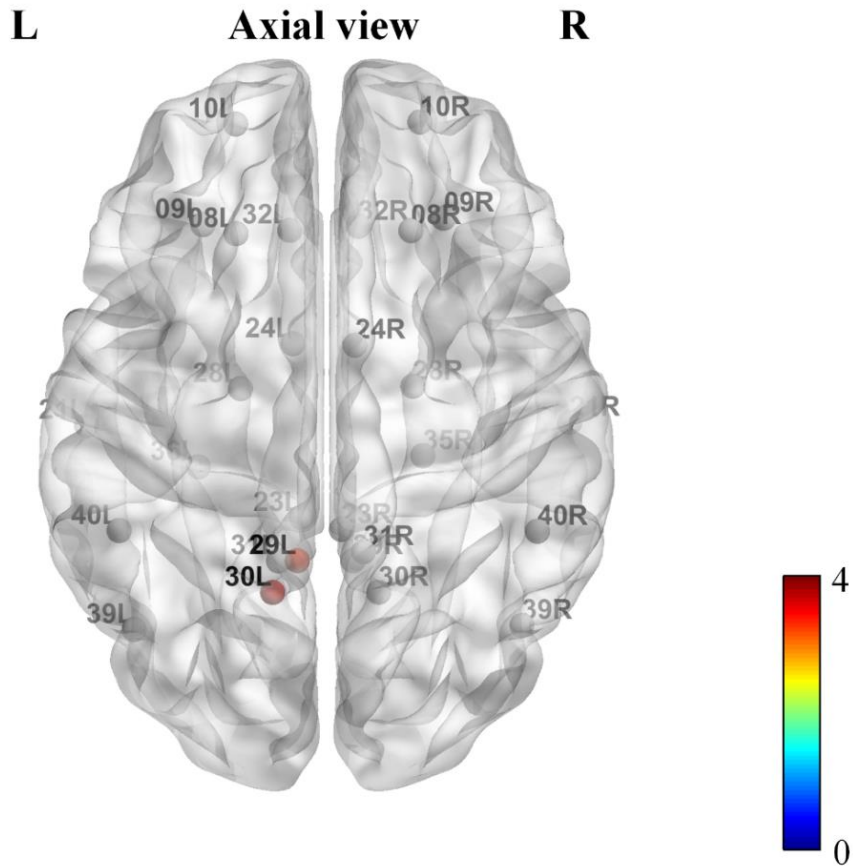
Figure 9. The theta phase-gamma amplitude couplings (TGC) which showed significant group difference between patients with first episode psychosis and healthy individuals after false discovery rate (FDR) correction. Color bar on the right side indicates t-value of group comparison. The gray color ROIs showed no significant differences. L, Left; R, Right.

Table 3. Comparison of theta-gamma coupling (TGC) between first episode psychosis and healthy control groups.

TGC of intra-ROI	t	P_{FDR}
BA08L	0.559	0.674
BA09L	0.205	0.838
BA10L	1.711	0.326
BA21L	-0.289	0.802
BA28L	-0.689	0.600
BA36L	0.733	0.600
BA23L	1.353	0.358
BA24L	1.396	0.357
BA32L	0.688	0.600
BA29L	3.303	0.018*
BA30L	4.120	0.002*
BA31L	1.433	0.357
BA39L	1.695	0.326
BA40L	1.485	0.357
BA08R	0.360	0.775
BA09R	0.988	0.455
BA10R	1.600	0.350
BA21R	2.102	0.177
BA28R	1.303	0.360
BA35R	1.434	0.357
BA23R	1.241	0.360
BA24R	1.177	0.362
BA32R	1.237	0.360
BA29R	2.716	0.054
BA30R	2.198	0.169
BA31R	1.167	0.362
BA39R	2.811	0.054
BA40R	0.485	0.704

Abbreviations: ROI, region of interest; FDR, false discovery rate; BA, Brodmann area; L, Left; R, right. *: $P < 0.05$.

Correlation analysis results

Partial correlation analysis controlling for the effect of age and sex was performed to examine the relationship of TGC in DMN with symptomatic severity or cognitive functioning in patients with FEP. Because higher TGC in FEP patients compared to HCs was observed at the left PCC, averaged TGC values of the BA29L and the BA30L were used as TGC values for correlation analysis. TGC of the left PCC showed significant correlation with the performance of TMT-A ($R = -0.44$, $P_{FDR} = 0.020$; Figure 10), TMT-B ($R = -0.35$, $P_{FDR} = 0.032$; Figure 11), immediate recall ($R = 0.36$, $P_{FDR} = 0.028$; Figure 12) and delayed recall ($R = 0.39$, $P_{FDR} = 0.028$; Figure 13) of CVLT. All other correlation analyses did not yield significant result after corrections for multiple comparisons.
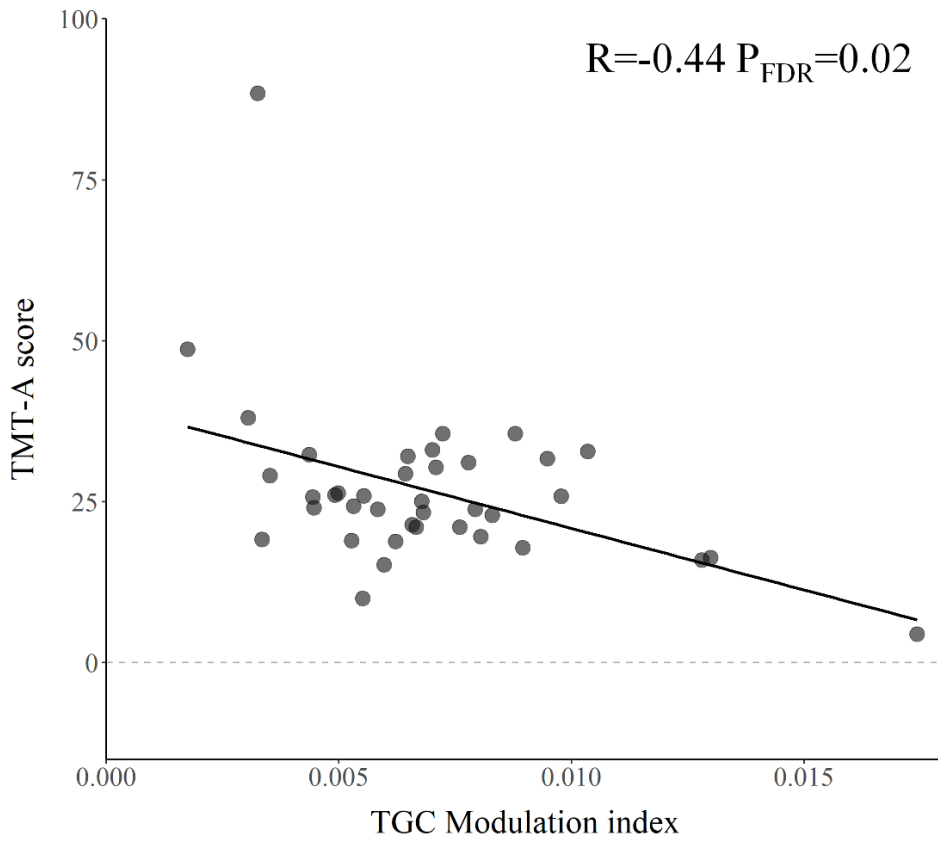
Figure 10. Correlation between the theta phase-gamma amplitude coupling (TGC) of the left posterior cingulate cortex (PCC) and the performance of Trail Making Test, Part A (TMT-A).
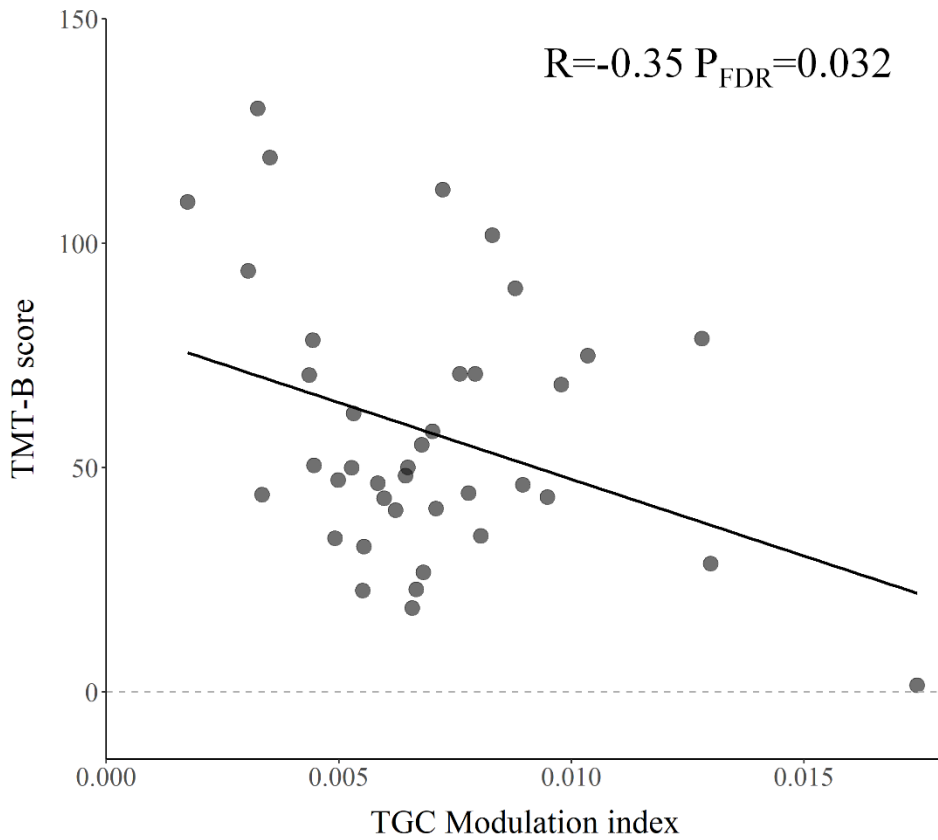
Figure 11. Correlation between the theta phase-gamma amplitude coupling (TGC) of the posterior cingulate cortex (PCC) and the performance of Trail Making Test, Part B (TMT-B).

Figure 12. Correlation between the theta phase-gamma amplitude coupling (TGC) of the posterior cingulate cortex (PCC) and the performance of California verbal learning test (CVLT), immediate recall.
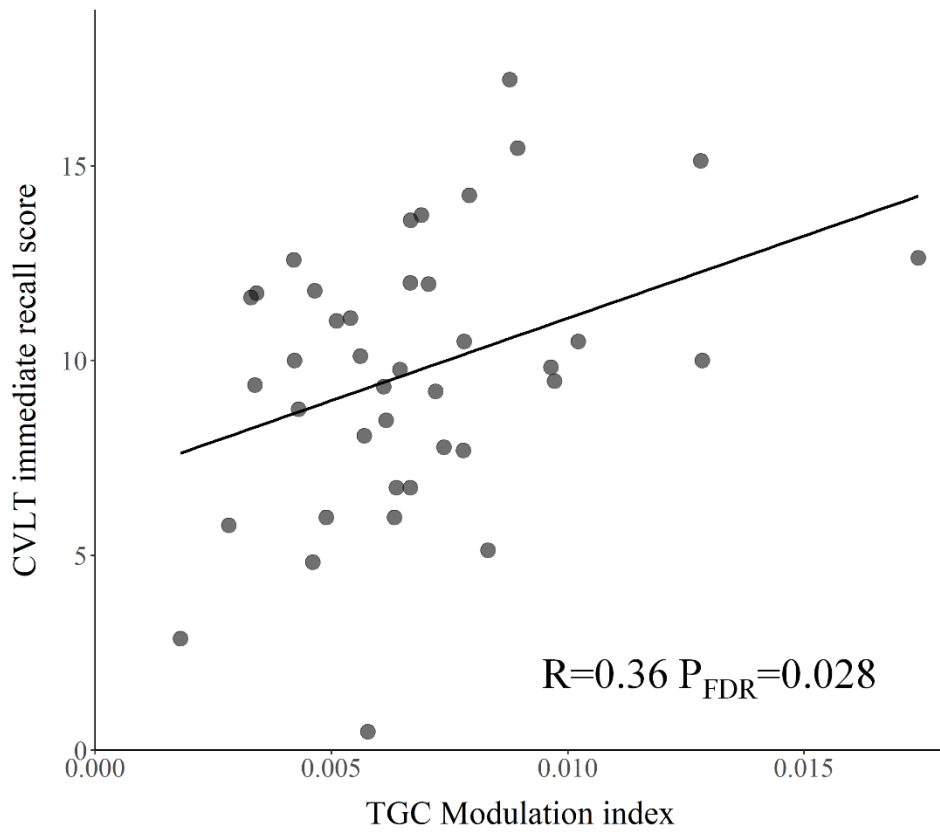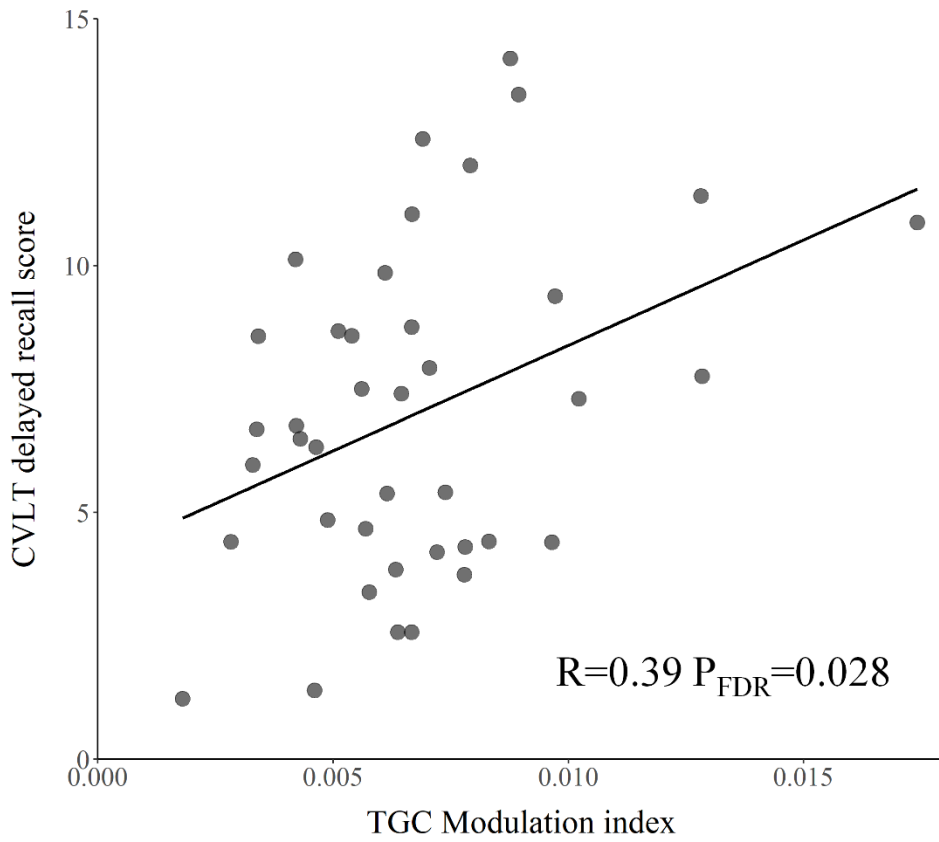
$R=0.39\ P_{FDR}=0.028$

Figure 13. Correlation between the theta phase-gamma amplitude coupling (TGC) of the posterior cingulate cortex (PCC) and the performance of California verbal learning test (CVLT), delayed recall.

Chapter 4. Discussion

Summary

In this study, TGCs of the resting-state EEG in the DMN-related brain areas were analyzed and compared between the FEP and HC groups to reveal neural correlates of altered information processing during the resting-state in patients with FEP. Patients with FEP showed larger TGC in the left PCC compared to HCs. In addition, larger TGC in the left PCC showed significant correlation with better performance in TMT-A and -B as well as immediate and delayed recall of CVLT. This study not only highlights the moment-by-moment neural underpinnings of cognitive dysfunction in FEP patients but also provides useful information in developing effective treatment methods for cognitive dysfunction of schizophrenia.
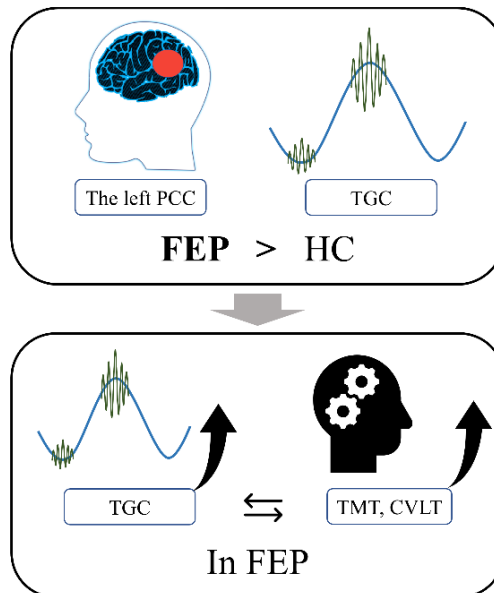
Figure 14. Summary of the results. FEP, first episode psychosis; HC, healthy controls; PCC, posterior cingulate cortex; TGC, theta phase-gamma amplitude coupling; TMT, Trail Making Test; CVLT, California verbal learning test.

Localized TGC in the DMN-related brain regions at the resting-state

After permutation test to confirm the presence of proper TGCs in the ROI combinations of DMN-related brain regions, we found 70 common ROI combinations in all participants. The presence of intra-ROI TGCs was confirmed in all DMN ROIs, while 41 inter-ROI TGCs were located in the limbic lobe in the same hemisphere or between hemispheres and one inter-ROI TGC was found only between right limbic and temporal lobes (BA21R - BA35R). However, since these inter-TGCs are located at close proximity to each other, in particular the inter-hemispheric ROI TGCs in the mid-line of the brain, significant results may have been produced due to the volume conduction problem (Kim et al., 2014; Vanneste et al., 2018). Thus, most significant TGCs confirmed in this study were localized TGCs (i.e. intra-ROI TGCs).

Larger TGC in FEP patients in the left PCC

The resting-state TGC in the left PCC was larger in FEP patients compared to HCs. The PCC is a brain region comprising DMN and previous fMRI studies reported similar results: FC was larger in PCC compared to other brain regions during resting-state in patients with schizophrenia (Liu et al., 2012; Whitfield-Gabrieli et al., 2009). In line with the current results, Kim et al. reported that resting-state left PCC activity increased in schizophrenia patients (Kim et al., 2014). The role of PCC is to integrate and transmit information to various brain regions via complex and rich connections. It has been shown that the activity of PCC increased when internally-directed cognitive processing occurred, such as retrieval of autobiographical memories, future planning, or mind-wandering Therefore, the

larger TGC in FEP patients in PCC during resting-state found in this study may reflect compensatory hyperactivity of internally-directed cognitive processing which would prepare the brain for actual cognitive performance. In line with that interpretation, inapposite deactivation of PCC during goal-directed cognitive processing was observed in patients with inefficient cognitive functioning (Anticevic et al., 2012; Crone et al., 2011; Sonuga-Barke and Castellanos, 2007).

Correlation with NCFT results

Larger TGC in the PCC of FEP patients compared to HCs was positively correlated with better performance in TMT-A and -B as well as immediate and delayed recall of CVLT. This finding suggests that TGC in the resting-state may reflect cognitive functioning during task performance. Because larger TGC was found in FEP patients compared to HCs, one may speculate that larger TGC reflects pathological mechanisms so that TGC of FEP patients should show negative correlation with good performance of NCFT. However, our results indicate opposite direction of correlation and this may be due to the altered DMN function in the resting-state in patients with FEP.

A main function of DMN is preparation and modulation of the switching to cognitive functioning state from the resting-state, which indicates control or reallocation of cognitive resources for the actual task performance during the resting-state (Crittenden et al., 2015). For example, Smith et al. reported that the activity of PCC and anteromedial prefrontal cortex (i.e. DMN) increased in brief resting-states between tasks and also in restart trials after rest, indicating that DMN plays an important role in the switching from the resting-state to the task performance state (Smith et al., 2018). During the cognitive task performance state, FEP patients with

cognitive impairments showed reduced suppression in the PCC and mPFC compared to FEP patients without cognitive impairments, which also suggested that abnormal DMN functioning was related to cognitive performance (Zhou et al., 2016). Thus, in this study, patients with FEP who had larger TGCs in DMN-related brain areas (i.e. PCC) could partially compensate for altered DMN functioning and show better performance in the actual cognitive tasks. Similarly, while lower resting-state activity was associated with cognitive decline accompanied by normal aging, the elderly group who compensated for relatively higher cognitive functioning showed greater activity during the resting-state, which was associated with better performance in actual NCFTs (Finnigan and Robertson, 2011; Zhang et al., 2019).

TMT is associated with visual scan, psychomotor speed, and set-switching ability (Varjacic et al., 2018). In elderly individuals, resting-state theta band power was positively correlated with perceptual speed and executive functioning (Vlahou et al., 2014). Therefore, our results, which showed that larger TGC of the left PCC correlated with better TMT performance, may also reflect less impaired processing speed and executive functioning of FEP patients. In addition, the PCC has structural connectivity with hippocampus related to episodic memory retrieval (Maddock et al., 2001; Mesulam, 1998; Wagner et al., 2005). It was shown that resting-state FC of the PCC and the MPFC was related to better performance of semantic cognition tasks in healthy volunteers (Krieger-Redwood et al., 2016). Elderly persons who had similar memory function with middle-aged or younger persons also showed greater FC of DMN with the PCC seed which was associated with better performances in CVLT compared to a typical elderly group with cognitive decline accompanied with normal aging (Zhang et al., 2019). Therefore, the larger TGC of the left PCC found in the FEP group in this study may also reflect the better memory retrieval function

associated with better performance of CVLT.

TGC in the DMN-related brain regions during the resting-state in patients with FEP

TGC is one of the CFCs which has been extensively studied from rodents to humans as a neural mechanism of information processing both at the local and global level (Hyafil et al., 2015). With recent advances in computational neuroscience, TGC is also known as an important mechanism for the computational modeling of neural activity (Sotero, 2016). Resting-state is not a state of doing nothing, but a state of preparation to cope with changes in the external environment (Mantini et al., 2007). Thus, abnormal resting-state functioning can lead to inadequate responses to environmental changes (i.e. inefficient distribution or use of cognitive resources), resulting in overall cognitive dysfunctions (Karbasforoushan and Woodward, 2012; Sheffield and Barch, 2016). It is therefore important to investigate whether neural activity is working properly during the resting-state.

TGC abnormalities found in FEP patients may be due to the disruption of rhythmic neural oscillation caused by the dysfunctional inhibition. Gamma oscillations emerge from the coordinated interaction of excitation and inhibition system, and the magnitude of gamma oscillation is modulated by slower rhythms, in particular theta wave (Buzsáki and Wang, 2012). The hypofunctioning NMDA receptor (NMDAr) results in both increased gamma and decreased theta (Pittman-Polletta et al., 2015). Synchronization of the pyramidal cell produces gamma wave, in that the inhibitory perisomatic postsynaptic potentials affect more the neural synchronization than the dendritic excitatory postsynaptic potentials (Buzsáki and Wang, 2012). Dysfunctional NMDAr produces weak inhibitory synapses which

cause synchronization problems manifested with altered gamma oscillation (Uhlhaas and Singer, 2015; Whittington et al., 2011). Therefore, altered TGCs found in FEP patients may be due to abnormal NMDAr functioning, which causes a decrease in synchronization of gamma band activity.

TGC shows a tendency to increase as task difficulty increases and more cognitive abilities are used, especially during the working memory task performances (Axmacher et al., 2010; Park et al., 2013). In a genetic mouse model, increasing task difficulty or optogenetical interference of encoding were associated with increased TGC (Tamura et al., 2017). Therefore, higher TGC indicates that the patients with FEP have difficulties in performing basic cognitive functioning at the resting-state and need more neuronal resources than HCs. This may be thought as a compensatory mechanism for proper information processing for preparing better performance in actual cognitive tasks (Tamura et al., 2017).

Limitation

This study has several limitations. First, there was a statistically significant difference in the sex between FEP and HC. Although I used age and sex as covariates to control the effect of age and sex on the EEG parameters, age- and sex-matched HC group would have been required for more accurate results. Second, most patients with FEP in this study were administered antipsychotic medications, which may have influenced the neural activity represented as TGC. Nevertheless, considering that similar results were shown in a study that investigated neuroleptic naïve patients with schizophrenia (Won et al., 2018), we can assume that the medication effect on TGC may be small. Third, NCFT data were not available for some FEP patients, thus the correlation analysis results should be interpreted with caution.

Chapter 5. Conclusion

It has long been hypothesized that schizophrenia is caused by cognitive dysfunction, and research aiming to investigate neural correlates of cognitive dysfunction has been continuously performed. However, considering the fact that the resting state is crucial for the preparation of actual cognitive performance, moment-by-moment cognitive processing during the resting state in patients with schizophrenia has not yet been fully studied. To the best of my knowledge, I am the first to perform TGC analysis in DMN-related brain regions using resting-state EEG, and found that FEP patients showed larger TGC in the left PCC compared to HCs. Moreover, larger TGC of the PCC found in FEP patients was positively correlated with better performances in various domains of NCFTs. Therefore, the larger resting-state TGC found in the FEP group may compensate for the abnormal basic cognitive functioning for better neurocognitive performance. In particular, as the PCC has been reported as a brain region with complex and rich connections compared to other brain regions, the findings of the current study support the traditional hypothesis that schizophrenia is caused by a cognitive dysfunction reflected as abnormal neural oscillation. Therefore, TGC of the PCC during the resting-state may be used as a biomarker in developing effective treatment methods for cognitive dysfunction and in detecting treatment responses in patients with schizophrenia. The results of the current study not only support the dysconnection hypothesis of schizophrenia but also highlight TGC as a neurophysiological correlate of cognitive dysfunction in patients with schizophrenia.

Bibliography

Alptekin, K., Akvardar, Y., Kivircik Akdede, B. B., Dumlu, K., Işik, D., Pirinçci, F., Yahssin, S., and Kitiş, A. (2005). Is quality of life associated with cognitive impairment in schizophrenia? *Prog. Neuro-Psychopharmacology Biol. Psychiatry* 29, 239–244.

Anticevic, A., Cole, M. W., Murray, J. D., Corlett, P. R., Wang, X.-J., and Krystal, J. H. (2012). The role of default network deactivation in cognition and disease. *Trends Cogn. Sci.* 16, 584–592.

Axmacher, N., Henseler, M. M., Jensen, O., Weinreich, I., Elger, C. E., and Fell, J. (2010). Cross-frequency coupling supports multi-item working memory in the human hippocampus. *Proc. Natl. Acad. Sci.* 107, 3228–3233.

Barr, M. S., Rajji, T. K., Zomorrodi, R., Radhu, N., George, T. P., Blumberger, D. M., and Daskalakis, Z. J. (2017). Impaired theta-gamma coupling during working memory performance in schizophrenia. *Schizophr. Res.* 189, 104–110.

Bassett, D. S., Nelson, B. G., Mueller, B. A., Camchong, J., and Lim, K. O. (2012). Altered resting state complexity in schizophrenia. *Neuroimage* 59, 2196–2207.

Battaglia, F. P. (2004). Local sensory cues and place cell directionality: additional evidence of prospective coding in the hippocampus. *J. Neurosci.* 24, 4541–4550.

Bell, M. A., Cuevas, K., and Tech, V. (1992). Using EEG to study cognitive development: issues and practices. *Bell Fox Cuevas Bell* 13, 1–11.

Belouchrani, A., and Cichocki, A. (2000). Robust whitening procedure in blind source separation context. *Electron. Lett.* 36, 2050–2051.

Benchenane, K., Peyrache, A., Khamassi, M., Tierney, P. L., Gioanni, Y., Battaglia, F. P., and Wiener, S. I. (2010). Coherent theta oscillations and reorganization of spike timing in the hippocampal-prefrontal network upon learning. *Neuron* 66, 921–936.

Bluhm, R. L., Miller, J., Lanius, R. A., Osuch, E. A., Boksman, K., Neufeld, R. W. J., Théberge, J., Schaefer, B., Williamson, P., Theberge, J., Schaefer, B., and Williamson, P. (2007). Spontaneous low-frequency fluctuations in the BOLD signal in schizophrenic patients: anomalies in the default network. *Schizophr. Bull.* 33, 1004–1012.

Buckner, R. L., Andrews-Hanna, J. R., and Schacter, D. L. (2008). The brain's default network: anatomy, function, and relevance to disease. *Ann. N. Y. Acad. Sci.* 1124, 1–38.

Buzsáki, G., and Wang, X.-J. (2012). Mechanisms of gamma oscillations. *Annu. Rev. Neurosci.* 35, 203–225.

Cabral, J., Kringelbach, M. L., and Deco, G. (2014). Exploring the network dynamics underlying brain activity during rest. *Prog. Neurobiol.* 114, 102–131.

Canolty, R. T., and Knight, R. T. (2010). The functional role of cross-frequency coupling. *Trends Cogn. Sci.* 14, 506–515.

Chaumon, M., Bishop, D. V. M., and Busch, N. A. (2015). A practical guide to the selection of independent components of the electroencephalogram for artifact correction. *J. Neurosci. Methods* 250, 47–63.

Cole, M. W., Anticevic, A., Repovs, G., and Barch, D. (2011). Variable global dysconnectivity and individual differences in schizophrenia. *Biol. Psychiatry* 70, 43–50.

Crittenden, B. M., Mitchell, D. J., and Duncan, J. (2015). Recruitment of the default mode network during a demanding act of executive control. *Elife* 4, 1–12.

Crone, J. S., Ladurner, G., Höller, Y., Golaszewski, S., Trinka, E., and Kronbichler, M. (2011). Deactivation of the default mode network as a marker of impaired consciousness: an fMRI study. *PLoS One* 6, e26373.

Delorme, A., and Makeig, S. (2004). EEGLAB: An open source toolbox for analysis of single-trial EEG dynamics including independent component analysis. *J. Neurosci. Methods* 134, 9–21.

Finnigan, S., and Robertson, I. H. (2011). Resting EEG theta power correlates with cognitive performance in healthy older adults. *Psychophysiology* 48, 1083–1087.

Friston, K., Brown, H. R., Siemerkus, J., and Stephan, K. E. (2016). The dysconnection hypothesis (2016). *Schizophr. Res.* 176, 83–94.

Friston, K. J. (1998). The disconnection hypothesis. *Schizophr. Res.* 30,

115–125.

Goff, D. C., Hill, M., and Barch, D. (2011). The treatment of cognitive impairment in schizophrenia. *Pharmacol. Biochem. Behav.* 99, 245–253.

Greicius, M. D., Krasnow, B., Reiss, A. L., and Menon, V. (2003). Functional connectivity in the resting brain: a network analysis of the default mode hypothesis. *Proc. Natl. Acad. Sci.* 100, 253–258.

Gusnard, D. A., and Raichle, M. E. (2001). Searching for a baseline : functional imaging and the resting human brain. *Nat. Rev. Neurosci.* 2, 685–694.

He, B., Yang, L., Wilke, C., and Yuan, H. (2011). Electrophysiological imaging of brain activity and connectivity-challenges and opportunities. *IEEE Trans. Biomed. Eng.* 58, 1918–1931.

Hunt, M. J., Kopell, N. J., Traub, R. D., and Whittington, M. A. (2017). Aberrant network activity in schizophrenia. *Trends Neurosci.* 40, 371–382.

Hyafil, A., Giraud, A. L., Fontolan, L., and Gutkin, B. (2015). Neural cross-frequency coupling: connecting architectures, mechanisms, and functions. *Trends Neurosci.* 38, 725–740.

Jensen, O., and Colgin, L. L. (2007). Cross-frequency coupling between neuronal oscillations. *Trends Cogn. Sci.* 11, 267–269.

Kahn, R. S., and Keefe, R. S. E. E. (2013). Schizophrenia is a cognitive illness: time for a change in focus. *JAMA Psychiatry* 70, 1107–1112.

Karbasforoushan, H., and Woodward, N. D. (2012). Resting-state networks in schizophrenia. *Curr. Top. Med. Chem.* 12, 2404–2414.

Khanna, A., Pascual-Leone, A., Michel, C. M., and Farzan, F. (2015). Microstates in resting-state EEG: current status and future directions. *Neurosci. Biobehav. Rev.* 49, 105–113.

Kim, J., Delcasso, S., and Lee, I. (2011). Neural correlates of object-in-place learning in hippocampus and prefrontal cortex. *J. Neurosci.* 31, 16991–17006.

Kim, J. S., Shin, K. S., Jung, W. H., Kim, S. N., Kwon, J. S., and Chung, C. K. (2014). Power spectral aspects of the default mode network in schizophrenia: an MEG study. *BMC Neurosci.* 15, 104.

Krieger-Redwood, K., Jefferies, E., Karapanagiotidis, T., Seymour, R., Nunes, A., Ang, J. W. A., Majernikova, V., Mollo, G., and Smallwood, J. (2016). Down but not out in posterior cingulate cortex: deactivation yet functional coupling with prefrontal cortex during demanding semantic cognition. *Neuroimage* 141, 366–377.

Kwon, J. S., Byun, M. S., Lee, T. Y., and An, S. K. (2012). Early intervention in psychosis: insights from Korea. *Asian J. Psychiatr.* 5, 98–105.

Li, F., Liu, T., Wang, F., Li, H., Gong, D., Zhang, R., Jiang, Y., Tian, Y., Guo, D., Yao, D., and Xu, P. (2015). Relationships between the resting-state network and the P3: evidence from a scalp EEG study. *Sci. Rep.* 5, 15129.

Lisman, J., and Buzsáki, G. (2008). A neural coding scheme formed by the

combined function of gamma and theta oscillations. *Schizophr. Bull.*

34, 974–980.

Lisman, J. E., and Jensen, O. (2013). The θ-γ neural code. *Neuron* 77, 1002–

1016.

Liu, H., Kaneko, Y., Ouyang, X., Li, L., Hao, Y., Chen, E. Y. H., Jiang, T.,

Zhou, Y., and Liu, Z. (2012). Schizophrenic patients and their

unaffected siblings share increased resting-state connectivity in the

task-negative network but not its anticorrelated task-positive network.

Schizophr. Bull. 38, 285–294.

Lynn, P. A., and Sponheim, S. R. (2016). Disturbed theta and gamma

coupling as a potential mechanism for visuospatial working memory

dysfunction in people with schizophrenia. *Neuropsychiatr.*

Electrophysiol. 2, 7.

Maddock, R. J., Garrett, A. S., and Buonocore, M. H. (2001). Remembering

familiar people: the posterior cingulate cortex and autobiographical

memory retrieval. *Neuroscience* 104, 667–676.

Mantini, D., Perrucci, M. G., Del Gratta, C., Romani, G. L., and Corbetta,

M. (2007). Electrophysiological signatures of resting state networks in

the human brain. *Proc. Natl. Acad. Sci. U. S. A.* 104, 13170–13175.

Mason, M. F., Norton, M. I., Van Horn, J. D., Wegner, D. M., Grafton, S.

T., and Macrae, C. N. (2007). Wandering minds: the default network

and stimulus-independent thought. *Science* 315, 393–395.

Meier, M. H., Caspi, A., Reichenberg, A., Keefe, R. S. E., Fisher, H. L., Harrington, H., Houts, R., Poulton, R., and Moffitt, T. E. (2014). Neuropsychological decline in schizophrenia from the premorbid to post-onset period: evidence from a population-representative longitudinal study. *Am. J. Psychiatry* 171, 91–101.

Mesholam-Gately, R. I., Giuliano, A. J., Goff, K. P., Faraone, S. V., and Seidman, L. J. (2009). Neurocognition in first-episode schizophrenia: a meta-analytic review. *Neuropsychology* 23, 315–336.

Mesulam, M. M. (1998). From sensation to cognition. *Brain* 121, 1013–1052.

Northoff, G., and Duncan, N. W. (2016). How do abnormalities in the brain's spontaneous activity translate into symptoms in schizophrenia? From an overview of resting state activity findings to a proposed spatiotemporal psychopathology. *Prog. Neurobiol.* 145–146, 26–45.

O'Leary, D. S., Flaum, M., Kesler, M. L., Flashman, L. A., Arndt, S., and Andreasen, N. C. (2000). Cognitive correlates of the negative, disorganized, and psychotic symptom dimensions of schizophrenia. *J. Neuropsychiatry Clin. Neurosci.* 12, 4–15.

Palm, U., Keeser, D., Hasan, A., Kupka, M. J., Blautzik, J., Sarubin, N., Kaymakanova, F., Unger, I., Falkai, P., Meindl, T., Ertl-Wagner, B., and Padberg, F. (2016). Prefrontal transcranial direct current stimulation for treatment of schizophrenia with predominant negative symptoms: a double-blind, sham-controlled proof-of-concept study.

Schizophr. Bull. 42, 1253–1261.

Pankow, A., Deserno, L., Walter, M., Fydrich, T., Bermpohl, F.,

Schlagenhauf, F., and Heinz, A. (2015). Reduced default mode

network connectivity in schizophrenia patients. *Schizophr. Res.* 165,

90–93.

Park, J. Y., Jhung, K., Lee, J., and An, S. K. (2013). Theta-gamma coupling

during a working memory task as compared to a simple vigilance task.

Neurosci. Lett. 532, 39–43.

Pettersson-Yeo, W., Allen, P., Benetti, S., McGuire, P., and Mechelli, A.

(2011). Dysconnectivity in schizophrenia: where are we now?

Neurosci. Biobehav. Rev. 35, 1110–1124.

Pittman-Polletta, B. R., Kocsis, B., Vijayan, S., Whittington, M. A., and

Kopell, N. J. (2015). Brain rhythms connect impaired inhibition to

altered cognition in schizophrenia. *Biol. Psychiatry* 77, 1020–1030.

Popov, T., Wienbruch, C., Meissner, S., Miller, G. A., and Rockstroh, B.

(2015). A mechanism of deficient interregional neural communication

in schizophrenia. *Psychophysiology* 52, 648–656.

Raichle, M. E., MacLeod, A. M., Snyder, A. Z., Powers, W. J., Gusnard, D.

A., and Shulman, G. L. (2001). A default mode of brain function. *Proc.*

Natl. Acad. Sci. 98, 676–682.

Raichle, M. E., and Mintun, M. A. (2006). Brain work and brain imaging.

Annu. Rev. Neurosci. 29, 449–476.

Sheffield, J. M., and Barch, D. M. (2016). Cognition and resting-state

functional connectivity in schizophrenia. *Neurosci. Biobehav. Rev.* 61, 108–120.

Smith, V., Mitchell, D. J., and Duncan, J. (2018). Role of the default mode network in cognitive transitions. *Cereb. Cortex* 28, 3685–3696.

Sonuga-Barke, E. J. S., and Castellanos, F. X. (2007). Spontaneous attentional fluctuations in impaired states and pathological conditions: a neurobiological hypothesis. *Neurosci. Biobehav. Rev.* 31, 977–986.

Sotero, R. C. (2016). Topology, cross-frequency, and same-frequency band interactions shape the generation of phase-amplitude coupling in a neural mass model of a cortical column. *PLOS Comput. Biol.* 12, e1005180.

Tamura, M., Spellman, T. J., Rosen, A. M., Gogos, J. A., and Gordon, J. A. (2017). Hippocampal-prefrontal theta-gamma coupling during performance of a spatial working memory task. *Nat. Commun.* 8, 2182.

Thatcher, R. W., North, D. M., and Biver, C. J. (2014). LORETA EEG phase reset of the default mode network. *Front. Hum. Neurosci.* 8, 529.

Tort, A. B. L., Komorowski, R., Eichenbaum, H., and Kopell, N. (2010). Measuring phase-amplitude coupling between neuronal oscillations of different frequencies. *J. Neurophysiol.* 104, 1195–1210.

Tort, A. B. L., Komorowski, R. W., Manns, J. R., Kopell, N. J., and Eichenbaum, H. (2009). Theta-gamma coupling increases during the learning of item-context associations. *Proc. Natl. Acad. Sci. U. S. A.* 106, 20942–20947.

Tripathi, A., Kar, S. K., and Shukla, R. (2018). Cognitive deficits in schizophrenia: understanding the biological correlates and remediation strategies. *Clin. Psychopharmacol. Neurosci.* 16, 7–17.

Ueoka, Y., Tomotake, M., Tanaka, T., Kaneda, Y., Taniguchi, K., Nakataki, M., Numata, S., Tayoshi, S., Yamauchi, K., Sumitani, S., Ohmori, T., Ueno, S. ichi, and Ohmori, T. (2011). Quality of life and cognitive dysfunction in people with schizophrenia. *Prog. Neuro-Psychopharmacology Biol. Psychiatry* 35, 53–59.

Uhlhaas, P. J., Haenschel, C., Nikolic, D., and Singer, W. (2008). The role of oscillations and synchrony in cortical networks and their putative relevance for the pathophysiology of schizophrenia. *Schizophr. Bull.* 34, 927–943.

Uhlhaas, P. J., and Singer, W. (2015). Oscillations and neuronal dynamics in schizophrenia: the search for basic symptoms and translational opportunities. *Biol. Psychiatry* 77, 1001–1009.

Unschuld, P. G., Buchholz, A. S., Varvaris, M., Van Zijl, P. C. M., Ross, C. A., Pekar, J. J., Hock, C., Sweeney, J. A., Tamminga, C. A., Keshavan, M. S., Pearlson, G. D., Thaker, G. K., and Schretlen, D. J. (2014). Prefrontal brain network connectivity indicates degree of both schizophrenia risk and cognitive dysfunction. *Schizophr. Bull.* 40, 653–664.

Urigüen, J. A., and Garcia-Zapirain, B. (2015). EEG artifact removal—state-of-the-art and guidelines. *J. Neural Eng.* 12, 31001.

Van Den Heuvel, M. P., and Pol, H. E. H. (2011). Exploring the brain
network: a review on resting-state fMRI functional connectivity.
Psiquiatr. Biol. 18, 28–41.

Vanneste, S., Song, J.-J., and De Ridder, D. (2018). Thalamocortical
dysrhythmia detected by machine learning. *Nat. Commun.* 9, 1103.

Varjacic, A., Mantini, D., Demeyere, N., and Gillebert, C. R. (2018). Neural
signatures of trail making test performance: evidence from lesion-
mapping and neuroimaging studies. *Neuropsychologia* 115, 78–87.

Vlahou, E. L., Thurm, F., Kolassa, I. T., and Schlee, W. (2014). Resting-
state slow wave power, healthy aging and cognitive performance. *Sci.
Rep.* 4, 33–36.

Wagner, A. D., Shannon, B. J., Kahn, I., and Buckner, R. L. (2005). Parietal
lobe contributions to episodic memory retrieval. *Trends Cogn. Sci.* 9,
445–453.

Wang, X.-J. (2010). Neurophysiological and computational principles of
cortical rhythms in cognition. *Physiol. Rev.* 90, 1195–1268.

Wang, X., Xia, M., Lai, Y., Dai, Z., Cao, Q., Cheng, Z., Han, X., Yang, L.,
Yuan, Y., Zhang, Y., Li, K., Ma, H., Shi, C., Hong, N., Szeszko, P.,
Yu, X., and He, Y. (2014). Disrupted resting-state functional
connectivity in minimally treated chronic schizophrenia. *Schizophr.
Res.* 156, 150–156.

Whitfield-Gabrieli, S., Thermenos, H. W., Milanovic, S., Tsuang, M. T.,
Faraone, S. V., McCarley, R. W., Shenton, M. E., Green, A. I., Nieto-

Castanon, A., LaViolette, P., Wojcik, J., Gabrieli, J. D. E., and Seidman, L. J. (2009). Hyperactivity and hyperconnectivity of the default network in schizophrenia and in first-degree relatives of persons with schizophrenia. *Proc. Natl. Acad. Sci.* 106, 1279–1284.

Whittington, M. A., Roopun, A. K., Traub, R. D., and Davies, C. H. (2011). Circuits and brain rhythms in schizophrenia: a wealth of convergent targets. *Curr. Opin. Pharmacol.* 11, 508–514.

Wilson, M. A., Mehta, M. R., and Lee, A. K. (2002). Role of experience and oscillations in transforming a rate code into a temporal code. *Nature*, 8–11.

Won, G. H., Kim, J. W., Choi, T. Y., Lee, Y. S., Min, K. J., and Seol, K. H. (2018). Theta-phase gamma-amplitude coupling as a neurophysiological marker in neuroleptic-naïve schizophrenia. *Psychiatry Res.* 260, 406–411.

Xia, M., Wang, J., and He, Y. (2013). BrainNet Viewer: a network visualization tool for human brain connectomics. *PLoS One* 8, e68910.

Yuan, H., Ding, L., Zhu, M., Zotev, V., Phillips, R., and Bodurka, J. (2016). Reconstructing large-scale brain resting-state networks from high-resolution EEG: spatial and temporal comparisons with fMRI. *Brain Connect.* 6, 122–135.

Zhang, J., Andreano, J. M., Dickerson, B. C., Touroutoglou, A., and Barrett, L. F. (2019). Stronger functional connectivity in the default mode and salience networks is associated with youthful memory in superaging.

Cereb. Cortex, 1–13.

Zhou, L., Pu, W., Wang, J., Liu, H., Wu, G., Liu, C., Mwansisya, T. E., Tao, H., Chen, X., Huang, X., Lv, D., Xue, Z., Shan, B., and Liu, Z. (2016). Inefficient DMN suppression in schizophrenia patients with impaired cognitive function but not patients with preserved cognitive function. *Sci. Rep.* 6, 21657.

Abstract in Korean

연구배경: 인지기능의 이상은 조현병 환자의 주요 병리적 원인 중 하나로 제안되었을 뿐만 아니라 환자들의 일상생활과 삶의 질에도 영향을 준다. 하지만 이것을 일으키는 신경생물학적 원인과 치료방법은 아직 명확하지 않다. 뇌의 휴식상태(Resting-state) 활동성은 인지기능을 효과적으로 사용하는데 주요한 요인이고, 뇌파는 고시간분해능으로 인지과정에서 일어나는 순간적인 신경활동을 측정할 수 있다. 따라서 본 연구에서는 휴식상태에서의 세타-감마 연결성 (Theta phase-gamma amplitude coupling)과 초발정신증(First episode psychosis) 환자의 인지기능 이상과의 관련성을 보고자 한다.

방법: 초발정신증 환자 59명과 건강한 대조군 50명을 대상으로 휴식 상태에서 눈을 감고 뇌파를 측정했다. 추가적으로 선로잇기검사(Trail making test) 파트 A, B와 캘리포니아 언어학습검사(California verbal learning test)를 이용해 인지기능을 측정했다. sLORETA를 이용해서 휴식상태의 디폴드모드네트워크(Default mode network)에서 일어나는 세타-감마 연결성 분석을 진행했다. 그리고 분석결과에 대한 그룹 간 비교 및 인지기능과의 상관성 분석을 진행했다.

결과: 초발정신증 환자와 대조군 비교결과 평균 세타-감마 연결성이 초발정신증 환자에게서 더 크게 나왔다. 영역별 분석 결과 초발정신증 군의 좌측 후대상피질(Posterior cingulate cortex)에서 세타-감마 연결성이 더 크게 나왔으며, 초발정신증 군의 후대상피질의 세타-감마 연결성이 높을수록 인지기능 수행능력이 우수한 상관관계를 보였다.

결론: 초발정신증 환자에게서 더 크게 측정된 휴식상태의 세타-감마 연결성은, 초발정신증 환자가 인지기능 전환 시 인지자원 재분배와 관련된 디폴트모드네트워크의 기능을 보상적으로 과활성화 시킨 상태로 볼 수 있다. 이 연구의 결과는 초발정신증 환자의 인지기능이상을 일으키는 신경활동의 순간적인 변화를 보았을 뿐만 아니라 조현병 환자의 인지기능 이상에 대한 원인 및 치료 방법에 대한 근거를 제시했다